Local rather than global H3K27me3 dynamics associates with differential gene expression in *Verticillium dahliae*

H. Martin Kramer[1], Michael F. Seidl[1,2], Bart P.H.J. Thomma[1,3,#,*], David E. Cook[1,4,#]

[1]Laboratory of Phytopathology, Wageningen University and Research, Droevendaalsesteeg 1, 6708 PB Wageningen, the Netherlands

[2]Theoretical Biology & Bioinformatics Group, Department of Biology, Utrecht University, Utrecht, The Netherlands

[3]University of Cologne, Institute for Plant Sciences, Cluster of Excellence on Plant Sciences (CEPLAS), 50674 Cologne, Germany

[4]Department of Plant Pathology, Kansas State University, 1712 Claflin Road, Manhattan, Kansas 66506, USA

[#]These authors contributed equally

[*]For correspondence: bthomma@uni-koeln.de

ABSTRACT

Differential growth conditions typically trigger global transcriptional responses in filamentous fungi. Such fungal responses to environmental cues involve epigenetic regulation, including chemical histone modifications. It has been proposed that conditionally expressed genes, such as those that encode secondary metabolites but also effectors in pathogenic species, are often associated with a specific histone modification, lysine27 methylation of H3 (H3K27me3). However, thus far no analyses on the global H3K27me3 profiles have been reported under differential growth conditions in order to assess if H3K27me3 dynamics governs differential transcriptional. Using ChIP- and RNA-sequencing data from the plant pathogenic fungus *Verticillium dahliae* grown in three *in vitro* cultivation media, we now show that a substantial number of the identified H3K27me3 domains globally display stable profiles among these growth conditions. However, we do observe local quantitative differences in H3K27me3 ChIP-seq signal that associate with a subset of differentially transcribed genes between media. Comparing the *in vitro* results to expression during plant infection suggests that *in planta*-induced genes may require chromatin remodelling to achieve expression. Overall, our results demonstrate that some loci display H3K27me3 dynamics associated with concomitant transcriptional variation, but many differentially expressed genes are associated with stable H3K27me3 domains. Thus, we conclude that while H3K27me3 is required for transcriptional repression, it does not appear that transcriptional activation requires global erasure of H3K27me3. We propose that the H3K27me3 domains that do not undergo dynamic methylation may contribute to transcription through other mechanisms or may serve additional genomic regulatory functions.

40 **INTRODUCTION**

41 The fungal kingdom comprises a plethora of species occupying an enormously diverse
42 range of ecological niches (1). As environments are typically dynamic, including the
43 effects of daily and yearly cycles, fungi continuously need to respond and adapt to
44 survive (2, 3). To this end, fungi have evolved various mechanisms to monitor their
45 environment and to transcriptionally respond to environmental cues (4). For instance, the
46 yeast *Saccharomyces cerevisiae* senses cold stress by increased membrane rigidity,
47 which leads to transcription of genes that, among others, encode cell damage-preventing
48 proteins (5). Furthermore, *S. cerevisiae* senses the quantitative availability of carbon and
49 nitrogen sources in the environment to determine which developmental program
50 maximises the potential for survival (6). In animal systems, epigenetic mechanisms (i.e.
51 those affecting genetic output without changing the genetic sequence) are implicated in
52 transcriptional responses to changing environments (7–9). Such epigenetic mechanisms
53 have similarly been proposed to contribute to environmental response in filamentous
54 fungi. For instance, the saprotrophic fungus *Neurospora crassa* phenotypically reacts to
55 environmental stimuli, such as changes in temperature and pH, yet *N. crassa* mutants
56 impaired in transcription-associated epigenetic mechanisms display reduced growth in
57 response to these stimuli (10). Similarly, the nectar-feeding yeast *Metschnikowia*
58 *reukaufii* and the ubiquitous fungus *Aureobasidium pullulans* fail to properly respond to
59 changing carbon sources when DNA methylation or histone acetylation are inhibited (11,
60 12). These results suggest that epigenetic mechanisms are important for transcriptional
61 responses to changing environments in diverse fungi, but many questions remain
62 regarding the precise mechanisms and function of epigenetic dynamics in fungi.

63 Epigenetic mechanisms, such as direct modifications of DNA and histone proteins
64 or physical changes to the chromatin architecture, can influence transcription by
65 regulating DNA accessibility (13). Chromatin that is accessible and potentially active is
66 termed euchromatin, while heterochromatin is condensed and often transcriptionally
67 silent (14). However, heterochromatic regions are not always repressed.
68 Heterochromatin is subcategorized into constitutive heterochromatin that remains

69 condensed throughout the cell cycle, and facultative heterochromatin that can de-
70 condense to allow transcription in response to developmental changes or to
71 environmental stimuli (15–17). In fungi, constitutive heterochromatin is often associated
72 with repeat-rich genome regions and is typically characterized by tri-methylation of lysine
73 9 on histone H3 (H3K9me3), while facultative heterochromatin is characterized by tri-
74 methylation of lysine 27 on histone H3 (H3K27me3) (18–21). Empirically, both H3K9me3
75 and H3K27me3 have been implicated in transcriptional regulation in various fungi (22,
76 23, 32, 24–31). The majority of these studies rely on genetic perturbation of the
77 enzymes that deposit methylation at H3K9 and H3K27, and the results consistently show
78 that depletion of methylation at these lysine residues mainly results in transcriptional
79 induction. However, as global depletion of a histone modification can result in pleiotropic
80 effects, such as improper localization of other histone modifications or altered
81 development (33, 34), it is difficult to infer transcriptional control mechanisms used for
82 natural gene regulation from these genetic perturbation experiments. Therefore,
83 additional research is needed to directly test the hypothesis that heterochromatin-
84 associated histone modifications directly regulate transcription either through their
85 dynamics, or their action to form or recruit transcriptional complexes (35–37).

86 The filamentous fungus *Verticillium dahliae* is a soil-borne broad host-range plant
87 pathogen that infects plants through the roots to invade the xylem vessels and cause
88 vascular wilt disease (38). Genomic and transcriptomic studies have revealed that the *V.*
89 *dahliae* genome harbours lineage-specific (LS) regions that are variable between strains
90 and enriched for genes that are *in planta* induced (39, 40). These LS regions are
91 generally considered genomic hotspots for evolutionary adaptation to plant hosts (39–
92 44). Recently we explored the epigenome of *V. dahliae* and distinguished LS regions from
93 the core genome based on particular chromatin signatures, including elevated levels of
94 H3K27me3 accompanied with accessible DNA and active transcription (44). Using a
95 machine learning approach and supported by orthogonal analyses, we identified nearly
96 twice as much LS DNA as previously considered, collectively referred to as adaptive
97 genomic regions (44). Given the elevated levels of H3K27me3 at adaptive genomic

98 regions in *V. dahliae*, and previous reports that removal of H3K27me3 results in
99 transcriptional induction (22–24), we now tested if H3K27me3 dynamics are required for
100 transcriptional activation of genes under different growth conditions. Ideally, the
101 involvement of H3K27me3 dynamics in differential gene expression of *V. dahliae* would
102 be studied between *in vitro* and *in planta* growth, as adaptive genomic regions are
103 enriched for *in planta* induced genes (40, 44). However, *V. dahliae* displays a low
104 pathogen-to-plant biomass during infection (45), which impedes technical procedures to
105 determine histone modification levels over the genome (46). Nevertheless, as H3K27me3
106 is generally reported to regulate transcription in response to environmental stimuli (15,
107 17), we hypothesize that it may be involved in transcriptional regulation in *V. dahliae*
108 during differential growth conditions *ex planta* as well. Here, we analyse RNA-seq, ChIP-
109 seq and ATAC-seq data of *V. dahliae* cultured in various axenic growth media to
110 understand if transcriptional dynamics require concomitant changes H3K27me3
111 modification status.
112
113 **RESULTS**
114 **Chromatin features correlate with gene expression levels**
115 To determine how general features of chromatin, such as histone modifications and DNA
116 accessibility, impact transcriptional activity in *V. dahliae*, we mapped the occurrence of
117 heterochromatic histone marks H3K9me3 and H3K27me3, euchromatic histone marks
118 H3K4me2 and H3K27ac, and chromatin accessibility determined by assay for transposase
119 accessible chromatin followed by sequencing (ATAC-seq) (47) (Fig. 1A, Fig. S1).
120 Grouping the *V. dahliae* genes into five expression quintiles, from quintile 1 containing
121 the highest 20% expressed genes to quintile 5 with the 20% lowest expressed genes, we
122 are able to integrate histone modification profiles and transcriptional activity. Expressed
123 genes (quintiles 1-4) displayed low H3K4me2 and H3K27ac coverage upstream of the
124 transcription start site (TSS), followed by a steep increase of coverage over the start of
125 the gene that decreases over the gene body and increases again at the transcription end
126 site (TES) (Fig. 1B). The strength of the association corresponds to the level of

127 transcription, also within quintiles (Fig. S2). The low H3K4me2 and H3K27ac coverage
128 directly upstream of the TSS coincides with increased chromatin accessibility, where
129 higher expressed quintiles have more open DNA (Fig. 1B, Fig. S2). This chromatin profile
130 upstream of the TSS suggests occurrence of a nucleosome depleted region. There is little
131 evidence of H3K9me3 over gene bodies and *cis*-regulatory regions (Fig. 1B, Fig. S2),
132 which corroborates that H3K9me3 marks TEs in constitutive heterochromatic regions
133 such as the centromeres (18, 44, 48, 49). During cultivation in PDB, H3K27me3 is mainly
134 present on genes that are lowly or not expressed (quintile 4 and 5) (Fig. 1B, Fig. S2).
135 These results, and association between chromatin features and transcriptional activity,
136 are consistent with reports for other fungi (24, 27, 32).

137 To further analyse the association between H3K27me3 and gene expression, we
138 identified 3,186 genes covered by H3K27me3 peaks (see methods) from triplicate grown
139 *V. dahliae* in PDB. These 3,186 genes were separated into five expression quintiles as
140 previously described. Interestingly, we found that genes in H3K27me3 domains with
141 higher expression values (quintile 1 and 2) had higher H3K4me2 over the gene body,
142 more accessible promoters, and lower H3K27me3 values (Fig. 1C). This suggests that
143 genes in H3K27me3 domains are not uniformly repressed or heterochromatic, and there
144 appears to be a quantitative, rather than qualitative, association between H3K27me3
145 association and gene activity. Genes with a lower association to H3K27me3 may
146 represent loci that are not in a stable state under the tested conditions, where some cells
147 have a more euchromatic profile and other have a more heterochromatic profile. While
148 we cannot infer these details from the current data, it is clear that genes with lower
149 expression in PDB are generally marked with H3K27me3, have less H3K4me3, and have
150 less accessible DNA in the region of transcription initiation (i.e. their promoter).

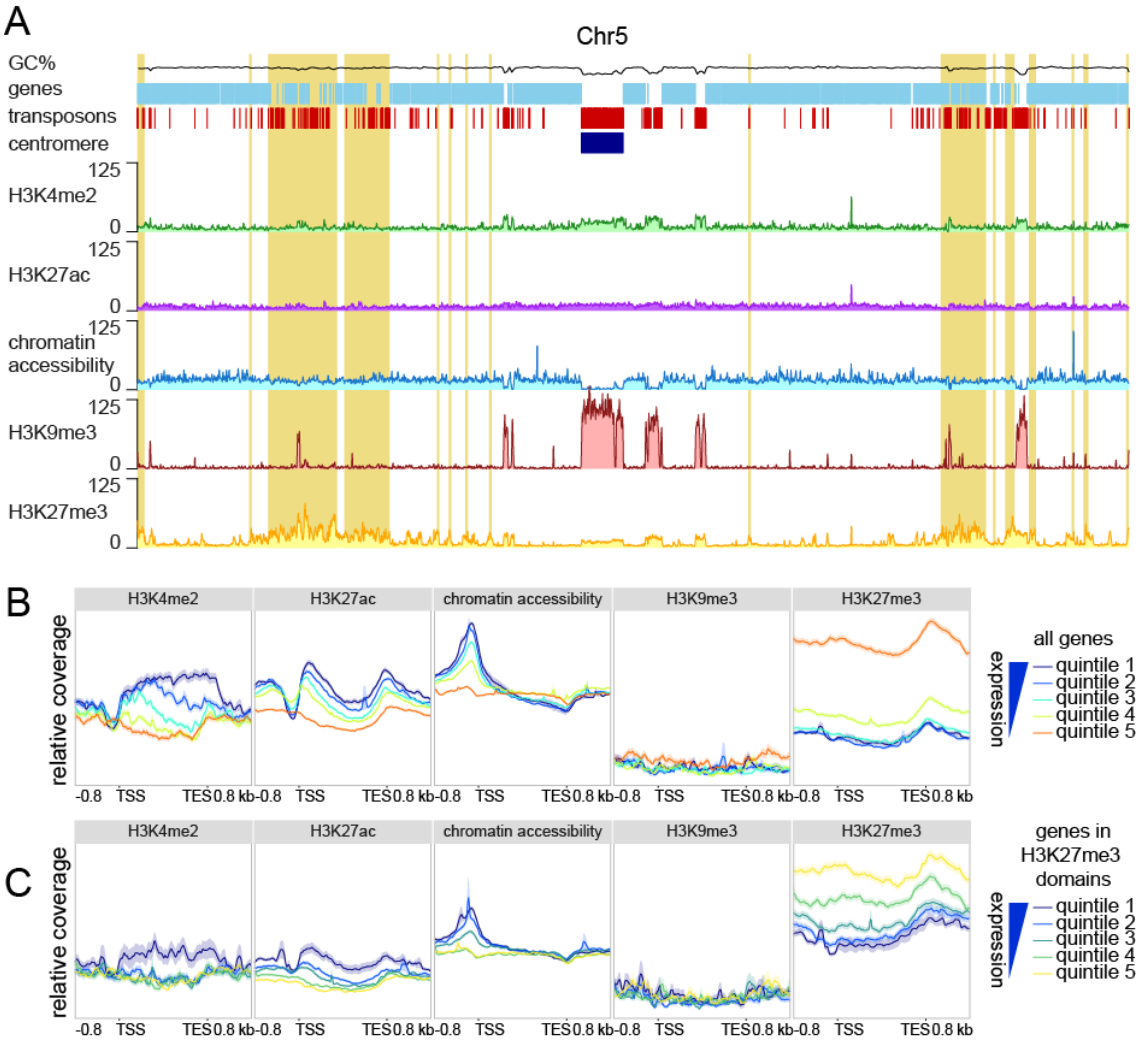

FIG 1. Lowly and non-expressed genes associate with H3K27me3. A) Whole genome distribution of the euchromatin-associated histone modification H3K4me2 and H3K27ac, the constitutive heterochromatin-associated histone modification H3K9me3, the facultative heterochromatin-associated histone modification H3K27me3 and chromatin accessibility as determined by ATAC-seq, based on chromosome 5 as an example. GC percentage is indicated in black, genes are indicated in light blue, transposons are indicated in red, the centromere is indicated in dark blue and adaptive genomic regions are indicated in yellow. B,C) Relative coverage of chromatin accessibility and the histone marks H3K4me2, H3K9me3, H3K27me3 over gene bodies (between transcription start site (TSS) and transcription end site (TES)) ±800 bp of flanking sequence, grouped into quintiles based on gene expression levels upon cultivation for six days potato dextrose broth (PDB), for (B) all genes, and for (C) all genes located in an H3K27me3 domain.

Genetic perturbation of H3K27me3 induces transcription of many genes that are differentially expressed *in vitro* and *in planta*

To further characterize the influence of H3K27me3 on gene expression in *V. dahliae*, we deleted the histone methyltransferase component of the Polycomb Repressive Complex 2 (PRC2), termed *Set7* (Δ*Set7*), leading to loss of H3K27me3 (Fig. 2A, Fig. S3, S4). We do note that some background signal is present for the H3K27me3-ChIP-seq conducted in

169 Δ*Set7*, but the signal is relatively uniform across the genome and does not correspond to
170 the regions of H3K27me3 found in wild-type (Fig. 2A). As H3K27me3 is generally
171 associated with facultative heterochromatin, we anticipated that the loss of H3K27me3
172 would mainly lead to induction of genes that were located in H3K27me3 domains in wild-
173 type *V. dahliae*. Out of the 839 genes that are induced in Δ*Set7* ($\log_2$-fold change >2,
174 $p<0.05$), 625 (74.5%) locate in H3K27me3 domains, which is significantly higher than
175 expected given that only 27.9% of genes locate in H3K27me3 domains (Fisher's exact
176 test, $p<0.00001$). In contrast, we find that 211 (27.6%) of 765 repressed genes in Δ*Set7*
177 are in H3K27me3 domains (no association, Fisher's exact test, $p=0.94$) (Fig. 2B,C).
178 Additionally, when comparing $\log_2$-fold changes in expression between Δ*Set7* and the
179 wild type strain, we observed that genes located in a H3K27me3 domain in wild type are
180 more significantly induced in Δ*Set7* than genes not locating in H3K27me3 domains (Two-
181 sample Student's T-test, $p<0.001$) (Fig. S5). These findings support the role of
182 H3K27me3 in transcriptional repression, and show that loss of H3K27me3 can lead to de-
183 repression during growth *in vitro*.

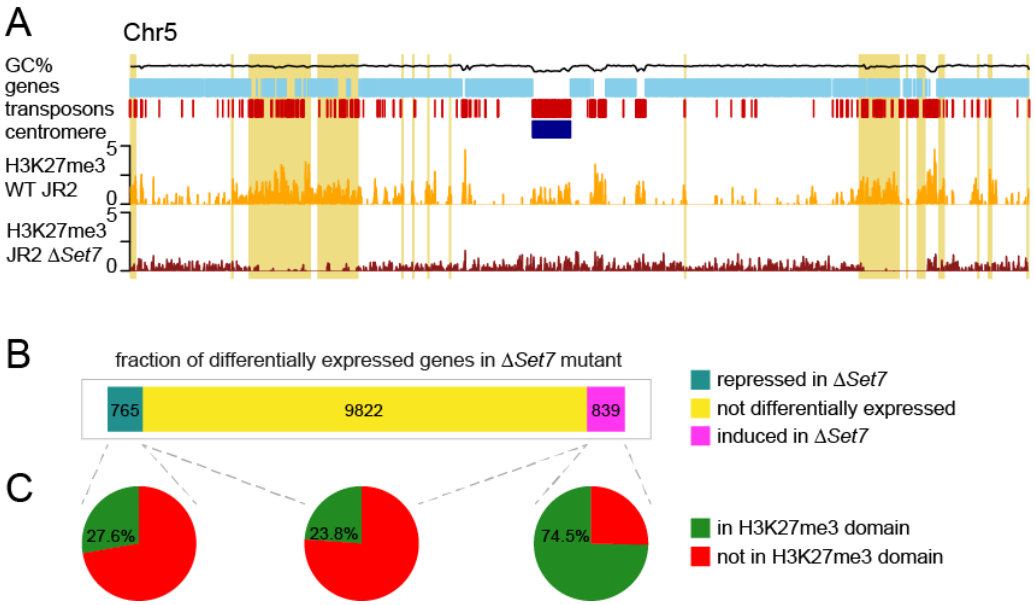

184

185 FIG 2. Genetic perturbation of H3K27me3 results in induction of genes that are transcriptionally
186 regulated in different growth conditions. A) H3K27me3 ChIP sequencing on triplicate JR2 WT
187 (yellow) and duplicate Δ*Set7* (red) samples with coverage over chromosome 5 as an example.
188 Adaptive genomic regions are indicated in yellow. B) Fractions of induced (log2 fold change >1,
189 $p<0.05$) and repressed (log2 fold change <-1, $p<0.05$) genes and genes that are not differentially
190 expressed between wild-type and Δ*Set7* that (C) locate in H3K27me3 domains.

191 **H3K27me3 domains are globally stable between *in vitro* growth conditions**

192 Given that H3K27me3 domains contribute to transcriptional repression, a key question
193 concerns the status of H3K27me3 under growth conditions where the underlying genes
194 are transcribed. One hypothesis is that H3K27me3 is removed or lost under growth
195 conditions that activate gene expression, which would be noticeable as a change in
196 H3K27me3 ChIP-seq domains between *V. dahliae* growth conditions that lead to
197 differential expression. Here, the observed changes in H3K27me3 domains should be
198 associated with transcriptional differences of the underlying genes. An alternative
199 hypothesis is that H3K27me3 domain status does not change in accordance with
200 transcriptional activity, and the repressive effects of H3K27me3 are released through
201 alternative means. To test this hypothesis, we performed triplicates of H3K27me3 ChIP-
202 seq on *V. dahliae* cultivated for six days in MS and CZA, in addition to the previously
203 generated ChIP-seq data in PDB. Based on correlation between replicates (Fig. S6), we
204 decided to continue with 3 replicates of H3K27me3 ChIP data in PDB and 2 replicates
205 each of H3K27me3 ChIP data in CZA and MS. Control ChIP-input samples were used to
206 normalize H3K27me3 datasets and identify H3K27me3-domains in each of the three
207 growth media. We identified a total of 2,654 genes that were always present in
208 H3K27me3 domains, regardless of the *in vitro* growth media (Fig. 3A). Interestingly, the
209 2,654 genes present in stable H3K27me3 domains display significantly stronger
210 differential expression between all pair-wise media comparisons when compared with
211 non-marked genes in all three growth conditions (Fig. 3B). This suggests that differential
212 gene expression can occur without changes in global H3K27me3 coverage. We further
213 checked whether genes that are differentially expressed between *in vitro* growth media
214 are associated with H3K27me3 during cultivation in the growth medium with low
215 expression levels (Fig. S7). Interestingly, we observed that for all pair-wise comparison
216 between growth media, genes with higher log2 fold-changes in expression are more
217 likely to locate in an H3K27me3 domain in the non-transcriptionally permissive growth
218 medium (Fig. S7), again suggesting that H3K27me3 is involved in regulation of
219 differential gene expression. To assess if changes in H3K27me3 domains between the

220 media were associated with changes in transcription, we compared differences in
221 domains and differential gene expression between media. We first analysed differential
222 expression for genes present in H3K27me3 domains in two media but not in an
223 H3K27me3 domain in the third medium. For example, we identified 366 genes that were
224 in a H3K27me3 domain in PDB and MS but not during CZA growth (Fig. 3A), and found
225 that these genes are not differential expressed between PDB and MS (one-sample t-test,
226 p 0.99), but they are higher expressed in CZA compared to both PDB (one-sample t-test,
227 p 2e-4) and MS (one-sample t-test, p 5e-8) (Fig. 3C). Similarly, genes present in shared
228 H3K27me3 domains for CZA and PDB growth (111 genes) are not differentially expressed
229 between CZA and PDB (one-sample t-test, p 0.92) when the genes are associated with
230 H3K27me3, they are higher expressed in MS than in PDB (one-sample t-test, p 4e-3),
231 but not higher expressed in MS than CZA (one-sample t-test, p 0.99). For genes present
232 in shared H3K27me3 domains between MS and CZA growth (223 genes), we did not
233 observe statistically significant transcriptional differences between the growth conditions
234 where the genes lacked H3K27me3 domains (Fig. 4A, C). Analysing H3K27me3 domains
235 unique to a medium, we found that CZA growth had the greatest number and proportion
236 of unique genes locating in H3K27me3 domains (23.3%), followed by 8.0% unique to MS
237 growth, and 1.7% unique to PDB growth (Fig. 3A). The genes uniquely marked in any
238 condition did not show consistently increased expression in the condition in which the
239 gene was not located in an H3K27me3 domain (Fig 3D). Overall these results suggest
240 that differential expression can be associated with differential H3K27me3 domain status,
241 but it is not a requirement. We observed clear examples where the loss of H3K27me3 in
242 one medium is associated with increased transcription in that medium, but this was not
243 universally true. Many genes undergo differential gene expression between growth
244 conditions and remain in stable H3K27me3 domains. We note that the majority of genes
245 located in H3K27me3 domains were common to all three growth conditions, accounting
246 for 83.3%, 75.3% and 68.2% of the identified genes in H3K27me3 domains from PDB,
247 MS and CZA growth, respectively, indicating that the qualitative presence of H3K27me3
248 domains is globally stable.

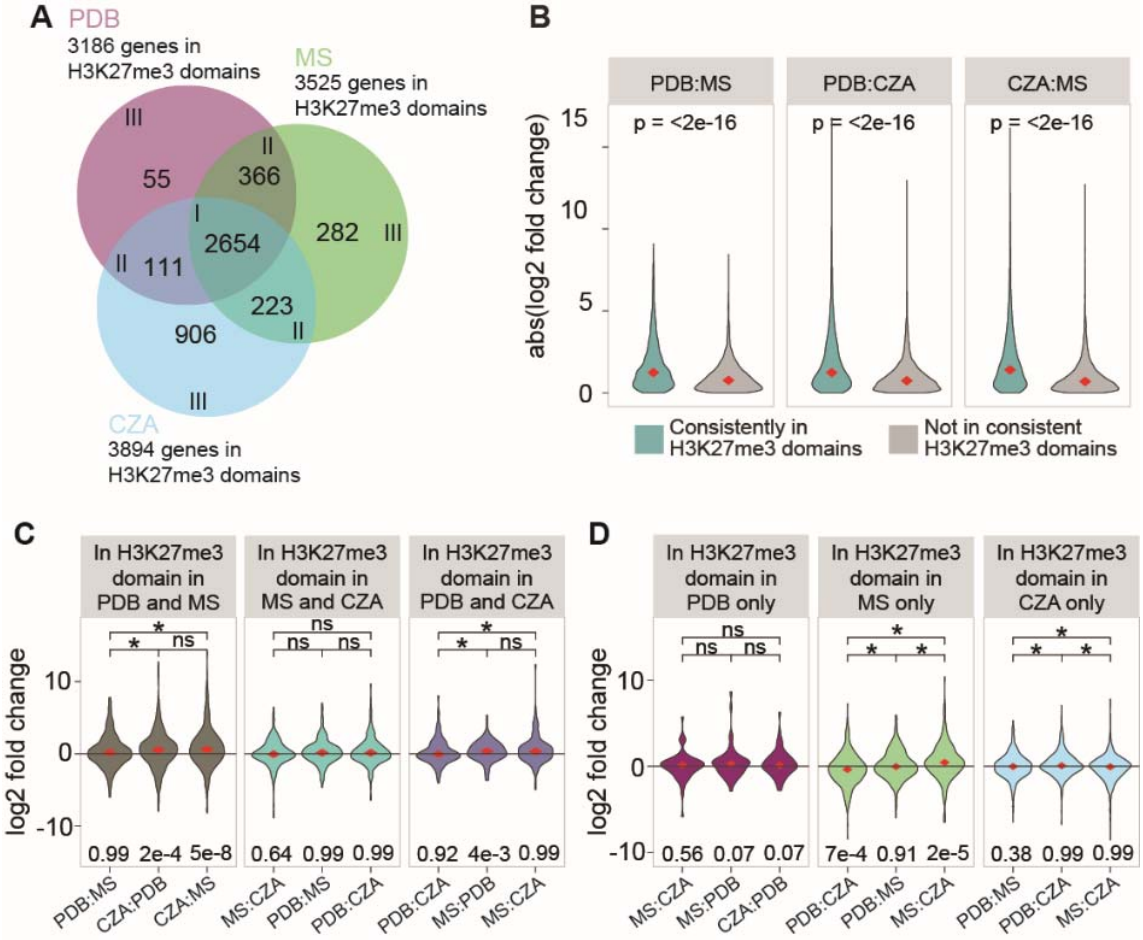

FIG 3. Differential H3K27 methylation partially explains differential expression. A) The number of genes located in H3K27me3 domains for *V. dahliae* cultivated for 6 days in Czapec-Dox (CZA), half-strength Murashige Skoog medium (MS) and potato dextrose broth (PDB). B) Absolute log2 fold-changes in expression between pairs of growth media. The genes were grouped between those consistently localized in H3K27me3 domains (2654 genes) and those not consistently present in H3K27me3 domains. C,D) Log2 fold-change values for each pair of growth medi1 for genes in H3K27me3 domains found in C) two or D) one of three tested *in vitro* growth media. Differential gene expression comparisons are set such that genes higher expressed in the medium in which they do not locate in H3K27me3 domain will have positive log2 fold-change. In case differential gene expression comparisons are between growth media in which the genes locate in H3K27me3 domains in C) both or D) neither of the compared media, the orientation of positive and negative log2 fold-change is arbitrary. Median values of violin plots are indicated with diamonds and shown above the plot. Significant difference of TPM values between growth media are determined with the One-Sample Wilcoxon Signed Rank Test (*: $p <= 0.05$). The one-sample two-sided T-test was used to test whether sample means significantly differ from 0, p-value shown below the plot.

Local quantitative differences in H3K27me3 levels are associated with transcriptional differences

Our analysis on H3K27me3 presence/absence dynamics did not account for potential quantitative differences between growth media. Whole chromosome plots of H3K27me3 domains identified between media reflect their generally stable presence (Fig. S8), but the analysis is based on qualitative H3K27me3 domain identification. Domain calling for

271 H3K27me3 results in broad domains, but this fails to capture higher resolution
272 quantitative differences that may exist between media, as is seen during inspection of
273 global chromosome plots (Fig. S8). To understand how qualitative domain calling impacts
274 the analysis, we examined quantitative differences between H3K27me3 ChIP-seq signal
275 and transcriptional output between pairs of growth conditions. Genes were grouped
276 based on differential gene expression between media, where genes that are significantly
277 higher expressed in media A were one group and genes significantly that are higher
278 expressed in media B another group. Subsequently, the H3K27me3 ChIP-seq signal
279 relative to the input samples were normalized and compared between both growth media
280 for the groups of differentially expressed genes (Fig. 4). Comparing results for PDB
281 versus MS, we see that genes that are higher expressed in MS have a significantly lower
282 MS H3K27me3 ChIP-signal versus the same genes from PDB ChIP (Fig. 4A). The
283 contrasting comparison, genes that higher expressed in PDB, shows these genes do not
284 significantly differ in ChIP signal between PDB and MS growth (Fig. 4A). Further
285 integrating the transcriptional and ChIP fold-changes, for the 4,794 genes that have an
286 input-corrected H3K27me3 ChIP signal above 0 in either MS and PDB, we see that genes
287 higher expressed in PDB have a significantly lower log2 fold-change for H3K27me3
288 coverage, indicating these genes have lower H3K27me3-signal in PDB when compared
289 with MS (Fig. 4B). Quantifying the number of genes in quadrant II and IV, we find that
290 396 (242+154) display a negative association between transcription and H3K27me3
291 ChIP-signal, whereas 256 (145+111) display a positive association (Fig. 4B). Thus, more
292 genes are present in the quadrants that represent genes having lower H3K27me3 levels
293 and higher transcription between the two growth conditions. The linear regression based
294 on all genes is R=-0.1, also suggesting the low but significant negative association (Fig.
295 4B). It is clear that the association between differential expression and changes in ChIP-
296 signal is not true for all genes, but overall we observe that the majority of genes that
297 display changes for H3K27me3 ChIP-signal between media show the predicted
298 transcriptional response where less H3K27me3 is associated with higher transcription
299 (Fig. 4B).

300 Results for PDB versus CZA growth showed that genes higher expressed in CZA
301 have higher H3K27me3 levels in PDB, consistent with the expected association (Fig. 4C).
302 For genes higher expressed in PDB, however, we also observed a higher H3K27me3 level
303 in PDB. Globally, the data indicated that genes higher expressed in CZA have more
304 H3K27me3 ChIP signal in PDB than genes that are higher expressed in PDB, indicating a
305 negative association between transcription and H3K27me3 presence (Fig. 4D). This is
306 corroborated by the number of genes per quadrant, as 568 (197+371) genes locate in
307 quadrants II and IV, whereas 469 (112+357) genes locate in quadrants I and III (Fig.
308 4D). The linear regression analysis indicates a slight negative association between
309 differential expression and H3K27me3 ChIP-signal (Fig. 4D). We also observed an overall
310 higher ChIP-signal from samples grown in CZA, but the reason for this is not clear.
311 Results for CZA versus MS growth showed that genes higher expressed in CZA
312 had statistically higher levels of H3K27me3 ChIP-signal in MS medium, whereas genes
313 higher expressed in MS have higher levels of H3K27me3 in CZA medium (Fig. 4E). The
314 same pattern was observed in the integrated analysis, as genes higher expressed in CZA
315 have more H3K27me3 signal in MS (Fig. 4F). There are 812 (244+568) genes in
316 quadrant II and IV, supporting a negative association between differential transcription
317 and H3K27me3 ChIP-signal, whereas 387 (130+257) genes are present in quadrants I
318 and III. This is supported by the significant negative correlation (R=-0.23) (Fig. 4F).
319 Overall, the results of the integrated analyses show that there is an association between
320 quantitative transcriptional levels and H3K27me3 signal, where genes that are more
321 highly expressed in a transcriptionally permissive medium have less H3K27me3 when
322 compared with H3K27me3 levels in the repressive media. There are also many genes
323 that were differentially expressed without an accompanying shift in H3K27me3 log2 fold-
324 change (Fig. 4B,D,F). Collectively, these results are consistent with the observations of
325 the qualitative H3K27me3 presence/absence comparisons, and suggest that H3K27me3
326 levels are generally stable, but local changes at particular genes may contribute to
327 transcriptional dynamics.

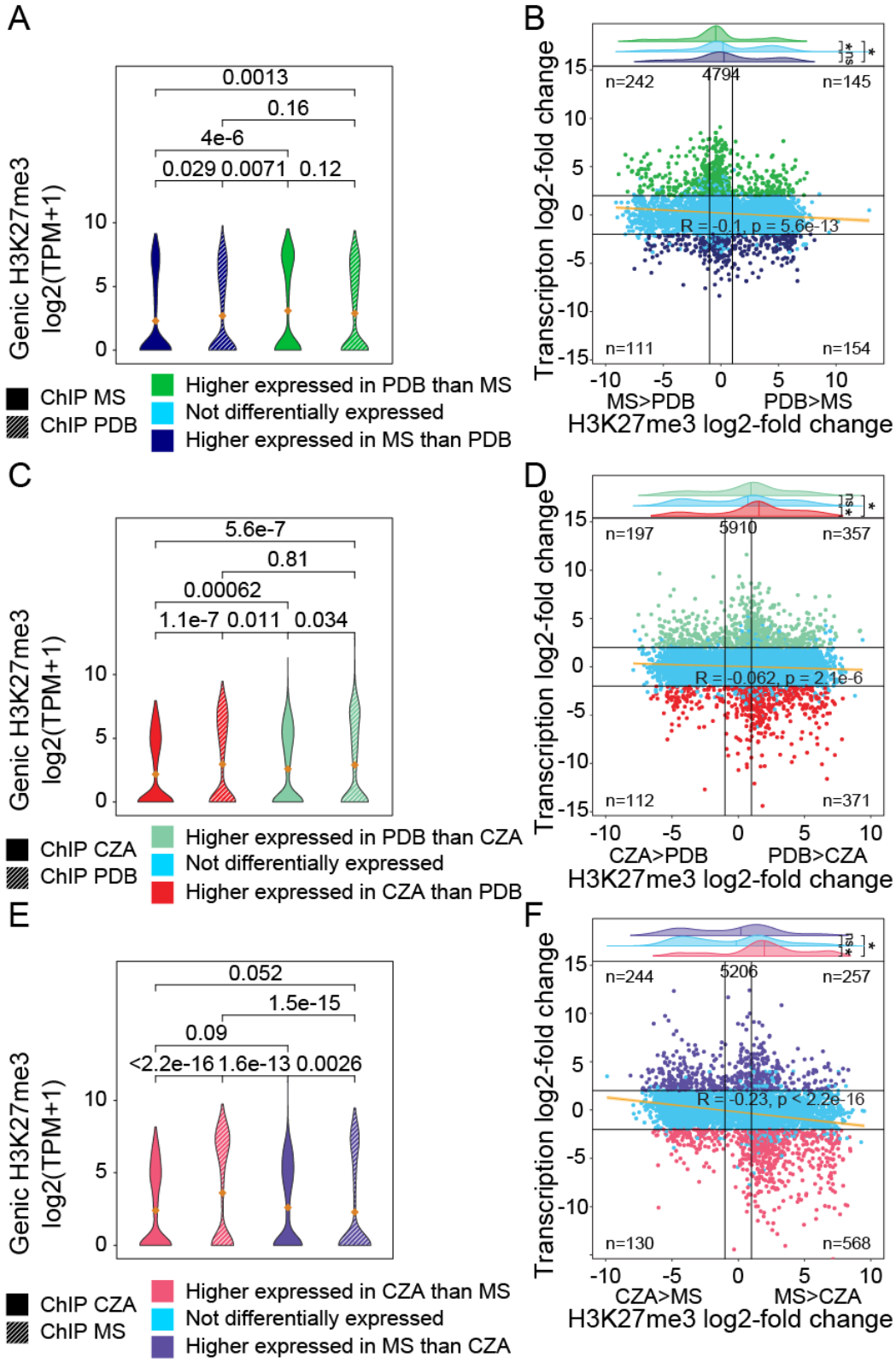

FIG 4. Differentially expressed genes associate with local changes in H3K27me3 coverage. Pairwise comparisons of input-corrected H3K27me3 coverage over differentially expressed genes for *V. dahliae* cultivated for 6 days in A,B) half-strength Murashige Skoog medium (MS) and potato dextrose broth (PDB), C,D) Czapec-Dox (CZA) and PDB, and E,F) MS and CZA. A,C,E) H3K27me3 coverage over differentially expressed genes in each corresponding growth medium. Mean values

334 of violin plots are indicated with orange diamonds. B,D,F) per gene comparison of log2-fold change
335 in transcription and genic H3K27me3 coverage, for genes with input-corrected H3K27me3 coverage
336 > 0 in either or both compared media (total number of genes indicated in top of plot). Black
337 horizontal lines indicate transcription log_2-fold change of -2 and 2, black vertical lines indicate
338 H3K27me3 log_2-fold change of -1 and 1. Numbers of genes in the four corner section are indicated.
339 Significant difference of TPM values between growth media or gene sets are determined with the
340 One-Sample Wilcoxon Signed Rank Test and indicated by their p-value or by asterisks (*: $p \leq 0.05$).

341 **Genes induced *in planta* are largely H3K27me3-associated across all tested**
342 **growth conditions**

343 The presented analyses compared the directionality of H3K27me3 and transcriptional
344 changes between axenic growth media to address if H3K27me3 dynamics are associated
345 with transcriptional dynamics. Another interesting growth condition for *V. dahliae* is host
346 colonization, and the contrast for the genes differentially expressed *in planta* when
347 compared with axenic culture. We have thus far been unable to perform ChIP on *V.*
348 *dahliae* during host colonization due to a low pathogen-to-plant biomass, and therefore
349 cannot compare H3K27me3 levels between these conditions. However, we can identify
350 the genes that are significantly induced during infection when compared with *in vitro*
351 growth media and assess their chromatin profiles in these media to assess if *in planta*-
352 induced genes appear heterochromatic during *in vitro* growth. Genes were grouped based
353 on differential expression between PDB and *in planta* growth and chromatin profiles
354 showed that genes that are higher expressed *in planta* had significantly more H3K27me3
355 during PDB growth when compared with genes that are more highly expressed in PDB
356 (Fig. 5A). These *in planta*-induced genes lacked H3K4me2 and the DNA was less
357 accessible during PDB growth (Fig. 5A). The association between *in planta* induction and
358 higher H3K27me3 levels was not only seen relative to PDB growth, but also to growth in
359 MS and CZA (Fig. 5B,C). For each media comparison, the genes that are more highly
360 expressed *in planta* have higher H3K27me3 levels during axenic growth. To understand
361 what genes are driving these differences, we investigated whether *in planta*-induced
362 genes that locate in H3K27me3 domains are overrepresented for genes that are
363 potentially involved in infection. There were approximately 600 genes that are more
364 highly expressed *in planta* when compared with any of the three media (Fig. 5D). We
365 found that, depending on the medium, from 41.2% to 52.8% of the *in planta*-induced

366 genes were located in H3K27me3 domains (Fig. 5D). We observed that the *in planta*-
367 induced genes within H3K27me3 domains have a higher, yet not statistically significant,
368 fraction of genes encoding secreted proteins or putative effectors when compared with all
369 *in planta*-induced genes. For example, genes in H3K27me3 domains that were *in planta*-
370 induced when compared with PDB growth (277 genes total), 15.5% had a secretion
371 signal and 4.3% were predicted effectors. This is compared to all *in planta*-induced genes
372 relative to PDB (673 genes total), where 12.3% had a secretion signal and 2.7% were
373 predicted effectors. These results were similar between the other two media, and we
374 conclude that *in planta*-induced genes in H3K27me3 domains have a slightly higher
375 fraction of genes that are potentially involved in infection when compared with *in planta*-
376 induced genes not in H3K27me3 domains. Collectively, these results indicate that genes
377 that are higher expressed *in planta* have a heterochromatic profile (i.e. H3K27me3
378 association, low H3K4me2, lower accessibility) when analysed in axenic culture. The
379 chromatin profile of these genes during *in planta* growth will need to be directly assessed
380 in the future.

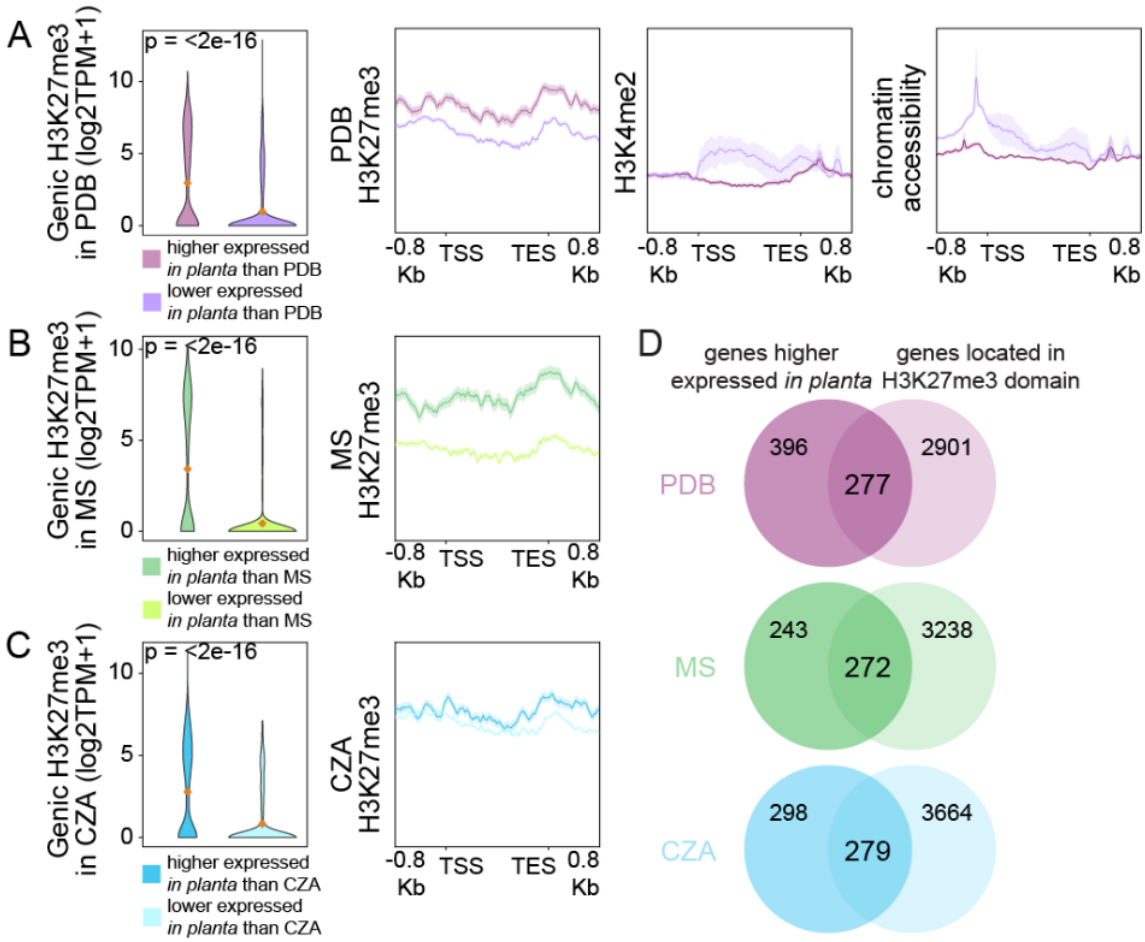

FIG 5. *In planta*-induced genes are H3K27me3-associated under transcriptionally repressive conditions. Violin plots display input-corrected H3K27me3 ChIP signal over genes differentially expressed between *in planta* and A) 6 days of cultivation in potato dextrose broth (PDB), B) half strength Murashige Skoog medium (MS), and C) Czapec-Dox medium (CZA). Mean values are indicated by orange diamonds. Line plots display average coverage of chromatin features over the gene sets. D) overlap of genes that are higher expressed *in planta* than in PDB, MS or CZA with genes located in an H3K27me3 domain in the corresponding growth medium. Significant differences of H3K27me3 coverage are determined with the One-Sample Wilcoxon Signed Rank Test (*: p <= 0.05).

DISCUSSION

Chemical histone modifications play an essential role in transcriptional regulation, but a number of mechanistic questions remain for their role in differential transcription in filamentous fungi. In this study, we show that many genes that are differentially transcribed between *in vitro* growth conditions are located in H3K27me3 domains. This is interesting because the mark contributes to transcriptional repression and it is relatively sparse in the genome, occupying approximately 33% of the genes. However, 35% to

398 70% of differentially expressed genes identified between growth conditions reside within
399 H3K27me3 domains. It is not clear what mechanism might drive this association.

400 The global fraction of genes that locates in H3K27me3 domains in *V. dahliae* is
401 similar to what has been reported for the asocomycete *Podospora anserina* (28), but
402 higher than for *N crassa, Zymoseptoria tritici*, *Leptosphaeria maculans,* and *Magnaporthe*
403 *oryzae* (9-16% of genes in H3K27me3 domain) (20, 30, 32, 50). Previous reports
404 showed that H3K27me3 represses transcription of secondary metabolite clusters in
405 *Fusarium spp.* and in *Epichloe festucae*, and of effectors in *Z. tritici* and *M. oryzae* (22,
406 24, 31, 32, 50). However, these reports have mainly relied on genomic association with
407 H3K27me3, genetic perturbation altering H3K27me3 deposition, and the analysis of only
408 few genes under natural conditions. Given our results, and these previous findings, our
409 hypothesis was that differences in transcription between *in vitro* growth conditions is in
410 part coordinated by dynamics for H3K27 methylation. We directly addressed this
411 phenomenon using genome-wide H3K27me3 profiling and RNA-seq under different *in*
412 *vitro* growth conditions. Consistent with reports in other fungi, we see that H3K27me3 is
413 associated with transcriptional repression, and that deleting *Set7*, encoding the histone
414 methyltransferase that is responsible for H3K27me3, led to induction of many genes
415 normally present in H3K27me3 domains. Importantly, our direct observations of
416 H3K27me3 levels and transcriptional output from three *in vitro* media showed that
417 H3K27me3 domains are generally stable globally. We see that 50% to 75% of the
418 identified H3K27me3 domains, depending on the medium analyzed, did not change
419 between the tested conditions. Despite many H3K27me3 domains not undergoing
420 presence/absence dynamics, numerous genes in these domains displayed differential
421 transcription between the tested conditions, indicating that complete loss of H3K27me3 is
422 not strictly required for transcriptional induction.

423 One possibility to account for these seemingly contradictory results is that even
424 though H3K27me3 appears stable at the level of broad-peak calling, there may be
425 smaller regions within the broad domain that are dynamic. Assessing quantitative
426 differences in H3K27me3 ChIP-seq levels at defined genomic locations between paired *in*

427 *vitro* growth conditions indicates that this can account for some of the observed
428 transcriptional differences. For example, some genes have a lower H3K27me3 ChIP-
429 signal upon growth in transcriptionally permissive medium when compared with growth
430 in a transcriptionally repressive medium. We interpret these results as evidence for local,
431 rather than global, changes in H3K27me3 dynamics contributing to transcriptional
432 regulation for the underlying genes. H3K27me3-associated genes that are differentially
433 expressed while presence of the histone mark remains stable, may be transcriptionally
434 regulated through the activity of H3K27me3 readers. For instance, the *Fusarium*
435 *graminearum* histone reader BP1, which is orthologous to *N. crassa* EPR-1, specifically
436 binds to H3K27me3 and co-represses gene transcription (51, 52). The gene encoding
437 BP1 is conserved within fungi, including *V. dahliae* (51). Dynamic binding of such
438 transcription-repressing histone reader to stable H3K27me3 domains may explain the
439 observed transcriptional dynamics.

440 We note that an individual histone does not permit for a quantitative tri-
441 methylation status, as an individual H3K27 is either tri-methylated or not. At the
442 nucleosome level, there can be none, one, or two H3K27 tails with a tri-methyl
443 modification. At the cell population level, there can be considerable quantitative
444 differences because of heterogeneity for histone modification status between individual
445 cells. Cell variability may be the source of quantitative differences observed in our
446 experiments, arising from variation for both the percent of cells with H3K27me3 and the
447 number of tails of a nucleosome with H3K27me3. While we cannot determine this based
448 on our present data, our results show that some genes that are differentially expressed
449 between growth conditions are associated with quantitative differences in H3K27me3
450 levels, providing evidence that chemical histone modifications dynamics can be involved
451 in a transcriptional regulatory mechanism in *V. dahliae*. The concept of local versus
452 global H3K27me3 changes is consistent with data from *M. oryzae*, in which direct *in*
453 *planta* H3K27me3 ChIP-qPCR showed that some, but not all, analyzed regions displayed
454 differential H3K27me3 levels consistent with increased transcription between *in planta*
455 and *in vitro* conditions (50). We have not been able to directly assess histone

456 modifications for *V. dahliae* during plant infection, but we did analyze the status of
457 H3K27 methylation during *in vitro* growth of *in planta*-induced genes. The *in planta*-
458 induced genes have significantly higher levels of H3K27me3 and the DNA is substantially
459 less accessible during *in vitro* growth when compared with genes that are highly
460 expressed during *in vitro* growth. We conclude that dynamics for H3K27me3 can
461 contribute to differential gene expression under natural conditions, but our results show
462 this is not required. Our conclusions are limited to the tested conditions, and it is possible
463 that analyzing H3K27me3 levels in different cell types or growth stages (e.g. spores,
464 microsclerotia, *in planta* infection) may yield a different picture of global H3K27me3
465 distribution. Additionally, our experiments focused on steady-state growth on different
466 media as these provide a clear and reproducible transcriptional difference. It is possible
467 that H3K27me3 dynamics occur rapidly in response to environmental changes, cues, or
468 developmental stages that we did not capture.

469 It appears evident that H3K27me3 contributes to additional genome functions
470 beyond strict transcriptional repression, at least in fungi (37). This is supported by our
471 data showing that the majority of H3K27me3 domains were stable between the tested
472 growth conditions, indicating these H3K27me3 domains have additional functions. Stable
473 H3K27me3 domains may represent another form of constitutive heterochromatin, but
474 this fact seems unlikely given that in our data many stable H3K27me3 domains harbored
475 differentially expressed genes between growth media. Additionally, results in *N. crassa*
476 have shown that genetic perturbation leading to the genome-wide loss of H3K9me3
477 causes a redistribution of H3K27me3 to previously H3K9me3 marked sites, but
478 interestingly, this re-distribution does not result in transcriptional silencing (53). Rather,
479 the redistribution of H3K27me3 in *N. crassa* lacking H3K9me3 appears to contribute to
480 genomic instability (53, 54). In *Z. tritici*, the enrichment of H3K27me3 at dispensable
481 chromosomes and empirical evidence that H3K27me3 somehow increases genomic
482 instability, additionally supports the hypothesis that H3K27me3 contributes to additional
483 genomic functions beyond transcriptional regulation (32, 48). Evolutionary analysis
484 across *Fusarium* and related species indicates that genes marked by H3K27me3 have a

485 higher duplication rate in *Fusarium* and are less conserved with more distantly related
486 species (55). Additional research is needed to fully understand the mechanisms of
487 H3K27me3 targeting, dynamics, and impact on genome stability in fungi. The results
488 presented here show that H3K27me3 domains are largely similar between *in vitro* growth
489 conditions, but that quantitative differences in H3K27me3 levels can be associated with
490 concomitant transcriptional differences between the tested conditions.

491 **MATERIALS AND METHODS**

492 **Fungal growth conditions**

493 *Verticillium dahliae* strain JR2 (CBS 143773; Faino et al., 2015) was cultured on potato
494 dextrose agar (PDA) (Oxoid, Thermo Scientific) at 22°C in the dark. Liquid cultures were
495 obtained by collecting conidiospores from PDA plates after approximately 2 weeks of
496 growth followed by inoculation at a final concentration of $1x10^4$ spores per mL into liquid
497 growth media. Media used in this study are potato dextrose broth (PDB) (Difco, Becton
498 Dickinson, Franklin Lakes, NJ, USA), half strength Murashige & Skoog plus vitamins (MS)
499 (Duchefa-Biochemie, Haarlem, The Netherlands) medium supplemented with 3%
500 sucrose, and Czapec-Dox medium (CZA) (Oxoid, Thermo Scientific, Waltham, MA, USA).
501 Liquid cultures were grown for 6 days in the dark at 22°C at 140 RPM. Mycelium was
502 collected by straining cultures through miracloth (22 µm) (EMD Millipore, Darmstadt,
503 Germany) and pressing to remove liquid after which the mycelium was flash frozen in
504 liquid nitrogen and ground to powder with a mortar and pestle. If required, samples were
505 stored at -20°C prior to nucleic acid extraction. All analyses were performed based on
506 triplicate cultures that were processed individually.

507

508 **RNA sequencing and analysis**

509 RNA was isolated from ground mycelium using TRIzol (Thermo Fisher Science, Waltham,
510 MA, USA) following manufacturer guidelines. Contaminating DNA was removed using the
511 TURBO DNA-free kit (Ambion, Thermo Fisher Science, Waltham, MA, USA) and RNA
512 integrity was assessed with gel-electrophoresis and quantified using a Nanodrop (Thermo
513 Fisher Science, Waltham, MA, USA). Library were prepared and singleend 50 bp
514 sequenced on the DNBseq platform at BGI (Hong Kong, China).

515 Sequencing reads were mapped to the reference annotation of *V. dahliae* strain
516 JR2 (56) using Kallisto quant (57) to calculate per gene TPM values. Differential
517 expression between cultivation in PDB and CZA, MS or during colonization of *Arabidopsis*
518 *thaliana* was determined using DESeq2 (58).

519

520 **ChIP-sequencing and analysis**

521 ChIP-seq was performed as described previously (Cook et al., 2020). Frozen ground
522 mycelium was added to ChIP lysis buffer, dounced 40 times and subsequently sonicated
523 for 5 rounds of 20 seconds with 40 second rest stages on ice. Supernatants were
524 collected after centrifugation and treated with MNase (New England Biolabs, Ipswich, MA,
525 United States) for 10 minutes in a 37°C waterbath. MNase activity was quenched by
526 addition of EGTA and samples were subsequently pre-cleared by addition of 40 µl Protein
527 A Magnetic Beads (New England Biolabs, Ipswich, MA, United States) and rotating at 4°C
528 for 60 min. Beads were captured and supernatant was divided over new tubes containing
529 antibodies against either H3K4me2, H3K9me3 or H3K27me3 (ActiveMotif; #39913,
530 #39765 and #39155) and incubated overnight with continuous rotation at 4°C.
531 Subsequently, the antibodies were captured, washed and nucleosomes were eluted from
532 beads, after which DNA was treated with Proteinase-K and cleaned-up using chloroform.
533 DNA was isolated by overnight precipitation in ethanol and DNA concentration was
534 determined with the Qubit™ dsDNA HS Assay Kit (Thermo Fisher Science, Waltham, MA,
535 USA). Sequencing libraries were generated using the TruSeq ChIP Library Preparation Kit
536 (Illumina, San Diego, CA, United States) according to instructions, but without gel
537 purification and with use of the Velocity DNA Polymerase (BioLine, Luckenwalde,
538 Germany) for 25 cycles of amplification. Single-end 125bp sequencing was performed on
539 the Illumina HiSeq2500 platform at KeyGene N.V. (Wageningen, the Netherlands).

540 Raw reads were trimmed using TrimGalore (59) and mapped to the *V.*
541 *dahliae* strain JR2 reference genome (56) using BWA-mem with default settings (60).
542 Three regions of the genome were masked due to aberrant mapping, (chr1:1-45000,
543 chr2:3466000-3475000, chr3:1-4200). ATAC-seq reads of *V. dahliae* cultured in PDB
544 (44) were treated similarly as ChIP-seq reads, but the paired end read pairs were
545 trimmed and mapped simultaneously, and only read-pairs <100 bp were considered for
546 further analyses, as these represent open DNA. Mapped reads were RPGC-normalized
547 using deepTools bamCoverage (61) with binsize 1,000 and smoothlength 3,000 for
548 plotting over the genome, and binsize 10 and smoothlength 30 for further analysis.

549 Normalized replicate samples with high correlation were selected and mean datasets per
550 growth media were generated with input controls for background signal correction using
551 WiggleTools mean (62). H3K27me3-enriched regions were determined on selected
552 replicates with input control using epic2 with a binsize of 2,500 bp (63). Average
553 coverage over gene bodies per expression quintile was calculated using deepTools
554 computeMatrix in scale-regions mode (61). Expression quintiles were generated by
555 sorting all genes based on their average TPM value from three replicates of *V. dahliae*
556 cultured for 6 days in PDB. We used deepTools multiBigwigSummary (61) to determine
557 the presence of H3K27me3 over gene bodies (region between TSS and TES) for each
558 replicate ChIP sample, as well as for input controls. Samples and input-controls were TPM
559 normalized, after which the normalized input-control signal was subtracted from
560 normalized H3K27me3 TPM values and resulting negative values were set to 0. Changes
561 in H3K27me3 levels between growth media were determined by taking the average
562 input-normalized H3K27me3 TPM values +1 and calculating the log2-fold change for each
563 pair-wise comparison.
564
565 **Generation of *Set7* deletion mutant**
566 The *Set7* deletion mutant (Δ*Set7*) was constructed as previously described (64). Briefly,
567 genomic DNA regions flanking the 5′ and 3′ ends of the coding sequences were amplified
568 with PCR using primers listed in Table S1 (primers 1-4) and cloned in to the pRF-HU2
569 vector (65) using USER enzyme following the manufacturer's protocol (New England
570 Biolabs, MA, USA). Sequence-verified vectors were transformed into *Agrobacterium*
571 *tumefaciens* strain AGL1 and used for *V. dahliae* conidiospore transformation as
572 described previously (64). *V. dahliae* transformants that appeared on hygromycin B were
573 transferred to fresh PDA supplemented with hygromycin B after five days. Putative
574 transformants were screened using PCR to verify deletion of the target gene sequence
575 and integration of the selection marker at the designated locus using primers listed in
576 Table S1 (primers 5-8). Analysis and comparison of gene expression in the *Set7* deletion
577 mutant to type *V. dahliae* was performed as described above.

578

579 **ACKNOWLEDGEMENTS**

580 This work was supported by a PhD grant of the Research Council Earth and Life Sciences
581 (project 831.15.002) to HMK, and by Human Frontier Science Program Postdoctoral
582 Fellowship (HFSP, LT000627/2014-L), by USDA's National Institute of Food and
583 Agriculture (award no. 2018-67013-28492) through the Plant Biotic Interactions
584 Program, and by the National Science Foundation (award no. 1936800) Division of
585 Molecular and Cellular Biosciences to DEC. Work in the laboratories of M.F.S and
586 B.P.H.J.T. is supported by the Research Council Earth and Life Sciences (ALW) of the
587 Netherlands Organization of Scientific Research (NWO). B.P.H.J.T acknowledges funding
588 by the Alexander von Humboldt Foundation in the framework of an Alexander von
589 Humboldt Professorship endowed by the German Federal Ministry of Education and
590 Research is furthermore supported by the Deutsche Forschungsgemeinschaft (DFG,
591 German Research Foundation) under Germany´s Excellence Strategy – EXC 2048/1 –
592 Project ID: 390686111.

593

594 **ADDITIONAL FILES**

595 Supplementary Figures

596 **Fig. S1.** Distribution of chromatin features over all chromosomes.

597 **Fig. S2.** Gene expression correlates with histone modification presence and chromatin
598 accessibility.

599 **Fig. S3.** Western blot shows loss of H3K27me3 in the *V. dahliae ΔSet7* deletion mutant.

600 **Fig. S4.** ChIP-sequencing shows loss of H3K27me3 in the *V. dahliae* ΔSet7 mutant.

601 **Fig. S5.** Genes associated with H3K27me3 in wild type *V. dahliae* are stronger
602 transcriptionally induced in the Δ*Set7* mutant than not H3K27me3 associated genes..

603 **Fig. S6.** Correlation between H3K27me3 ChIP samples

604 **Fig. S7.** Differentially expressed genes are enriched in H3K27me3 domains during
605 cultivation in the non-permissive growth medium.

606 **Fig. S8.** Distribution of H3K27me3 for V. dahliae cultivated in in vitro growth media.

607 Supplementary Tables

608 **Table S1.** Primers used to delete and analyse the *Set7* coding sequence in *V. dahliae*.

REFERENCES

1. Schmit JP, Mueller GM. 2007. An estimate of the lower limit of global fungal diversity. Biodivers Conserv 16:99–111.
2. Gibson G. 2008. The environmental contribution to gene expression profiles. Nat Rev Genet 9:575–581.
3. Selvig K, Alspaugh JA. 2011. pH response pathways in fungi: adapting to host-derived and environmental signals. Mycobiology 39:249–256.
4. Bahn Y-S, Xue C, Idnurm A, Rutherford JC, Heitman J, Cardenas ME. 2007. Sensing the environment: lessons from fungi. Nat Rev Microbiol 5:57–69.
5. Aguilera J, Randez-Gil F, Prieto JA. 2007. Cold response in *Saccharomyces cerevisiae*: new functions for old mechanisms. FEMS Microbiol Rev 31:327–341.
6. Schneper L, Düvel K, Broach JR. 2004. Sense and sensibility: nutritional response and signal integration in yeast. Curr Opin Microbiol 7:624–630.
7. Heijmans BT, Tobi EW, Stein AD, Putter H, Blauw GJ, Susser ES, Slagboom PE, Lumey LH. 2008. Persistent epigenetic differences associated with prenatal exposure to famine in humans. Proc Natl Acad Sci 105:17046–17049.
8. Zannas AS, Arloth J, Carrillo-Roa T, Iurato S, Röh S, Ressler KJ, Nemeroff CB, Smith AK, Bradley B, Heim C. 2015. Lifetime stress accelerates epigenetic aging in an urban, African American cohort: relevance of glucocorticoid signaling. Genome Biol 16:1–12.
9. Martin EM, Fry RC. 2018. Environmental influences on the epigenome: exposure-associated DNA methylation in human populations. Annu Rev Public Health 39:309–333.
10. Kronholm I, Johannesson H, Ketola T. 2016. Epigenetic control of phenotypic plasticity in the filamentous fungus *Neurospora crassa*. G3 Genes, Genomes, Genet 6:4009–4022.
11. Slepecky RA, Starmer WT. 2009. Phenotypic plasticity in fungi: a review with observations on *Aureobasidium pullulans*. Mycologia 101:823–832.
12. Herrera CM, Pozo MI, Bazaga P. 2012. Jack of all nectars, master of most: DNA methylation and the epigenetic basis of niche width in a flower-living yeast. Mol Ecol 21:2602–2616.
13. Slotkin RK, Martienssen R. 2007. Transposable elements and the epigenetic regulation of the genome. Nat Rev Genet 8:272–285.
14. Bannister AJ, Kouzarides T. 2011. Regulation of chromatin by histone modifications. Cell Res 21:381–395.
15. Trojer P, Reinberg D. 2007. Facultative heterochromatin: is there a distinctive molecular signature? Mol Cell 28:1–13.
16. Kim J-M, Sasaki T, Ueda M, Sako K, Seki M. 2015. Chromatin changes in response to drought, salinity, heat, and cold stresses in plants. Front Plant Sci 6:doi: 10.3389/fpls.2015.00114.
17. Wang J, Jia ST, Jia S. 2016. New insights into the regulation of heterochromatin. Trends Genet 32:284–294.
18. Lewis ZA, Honda S, Khlafallah TK, Jeffress JK, Freitag M, Mohn F, Schübeler D, Selker EU. 2009. Relics of repeat-induced point mutation direct heterochromatin formation in *Neurospora crassa*. Genome Res 19:427–437.
19. Lewis ZA, Adhvaryu KK, Honda S, Shiver AL, Knip M, Sack R, Selker EU. 2010. DNA methylation and normal chromosome behavior in *Neurospora* depend on five components of a histone methyltransferase complex, DCDC. PLoS Genet

657 6:e1001196.

658 20. Jamieson K, Rountree MR, Lewis ZA, Stajich JE, Selker EU. 2013. Regional control
659 of histone H3 lysine 27 methylation in *Neurospora*. Proc Natl Acad Sci 110:6027–
660 32.

661 21. Freitag M. 2017. Histone methylation by SET domain proteins in fungi. Annu Rev
662 Microbiol 71:413–439.

663 22. Chujo T, Scott B. 2014. Histone H3K9 and H3K27 methylation regulates fungal
664 alkaloid biosynthesis in a fungal endophyte-plant symbiosis. Mol Microbiol 92:413–
665 434.

666 23. Soyer JL, El Ghalid M, Glaser N, Ollivier B, Linglin J, Grandaubert J, Balesdent MH,
667 Connolly LR, Freitag M, Rouxel T, Fudal I. 2014. Epigenetic control of effector gene
668 expression in the plant pathogenic fungus *Leptosphaeria maculans*. PLoS Genet
669 10:e1004227.

670 24. Connolly LR, Smith KM, Freitag M. 2013. The *Fusarium graminearum* histone H3
671 K27 methyltransferase KMT6 regulates development and expression of secondary
672 metabolite gene clusters. PLoS Genet 9:e1003916.

673 25. Reyes-Dominguez Y, Boedi S, Sulyok M, Wiesenberger G, Stoppacher N, Krska R,
674 Strauss J. 2012. Heterochromatin influences the secondary metabolite profile in
675 the plant pathogen *Fusarium graminearum*. Fungal Genet Biol 49:39–47.

676 26. Wiemann P, Sieber CMK, von Bargen KW, Studt L, Niehaus EM, Espino JJ, Huß K,
677 Michielse CB, Albermann S, Wagner D, Bergner S V., Connolly LR, Fischer A,
678 Reuter G, Kleigrewe K, Bald T, Wingfield BD, Ophir R, Freeman S, Hippler M, Smith
679 KM, Brown DW, Proctor RH, Münsterkötter M, Freitag M, Humpf HU, Güldener U,
680 Tudzynski B. 2013. Deciphering the cryptic genome: genome-wide analyses of the
681 rice pathogen *Fusarium fujikuroi* reveal complex regulation of secondary
682 metabolism and novel metabolites. PLoS Pathog 9:e1003475.

683 27. Reyes-Dominguez Y, Bok JW, Berger H, Shwab EK, Basheer A, Gallmetzer A,
684 Scazzocchio C, Keller N, Strauss J. 2010. Heterochromatic marks are associated
685 with the repression of secondary metabolism clusters in *Aspergillus nidulans*. Mol
686 Microbiol 76:1376–1386.

687 28. Carlier F, Li M, Maroc L, Debuchy R, Souaid C, Noordermeer D, Grognet P,
688 Malagnac F. 2021. Loss of EZH2-like or SU (VAR) 3–9-like proteins causes
689 simultaneous perturbations in H3K27 and H3K9 tri-methylation and associated
690 developmental defects in the fungus *Podospora anserina*. Epigenetics Chromatin
691 14:1–28.

692 29. Lukito Y, Lee K, Noorifar N, Green KA, Winter DJ, Ram A, Hale TK, Chujo T, Cox
693 MP, Johnson LJ. 2021. Regulation of host-infection ability in the grass-symbiotic
694 fungus *Epichloë festucae* by histone H3K9 and H3K36 methyltransferases. Environ
695 Microbiol 23:2116–2131.

696 30. Soyer JL, Clairet C, Gay EJ, Lapalu N, Rouxel T, Stukenbrock EH, Fudal I. 2021.
697 Genome-wide mapping of histone modifications during axenic growth in two
698 species of *Leptosphaeria maculans* showing contrasting genomic organization.
699 Chromosom Res 29:219–236.

700 31. Studt L, Rösler SM, Burkhardt I, Arndt B, Freitag M, Humpf HU, Dickschat JS,
701 Tudzynski B. 2016. Knock-down of the methyltransferase Kmt6 relieves H3K27me3
702 and results in induction of cryptic and otherwise silent secondary metabolite gene
703 clusters in *Fusarium fujikuroi*. Environ Microbiol 18:4037–4054.

704 32. Möller M, Schotanus K, Soyer JL, Haueisen J, Happ K, Stralucke M, Happel P, Smith
705 KM, Connolly LR, Freitag M, Stukenbrock EH. 2019. Destabilization of chromosome
706 structure by histone H3 lysine 27 methylation. PLoS Genet 15:e1008093.

707 33. Tian L, Chen ZJ. 2001. Blocking histone deacetylation in *Arabidopsis* induces

708 pleiotropic effects on plant gene regulation and development. Proc Natl Acad Sci
709 98:200–205.

710 34. Fan A, Mi W, Liu Z, Zeng G, Zhang P, Hu Y, Fang W, Yin W-B. 2017. Deletion of a
711 histone acetyltransferase leads to the pleiotropic activation of natural products in
712 Metarhizium robertsii. Org Lett 19:1686–1689.

713 35. Galazka JM, Freitag M. 2014. Variability of chromosome structure in pathogenic
714 fungi-of "ends and odds." Curr Opin Microbiol 20:19–26.

715 36. Seidl MF, Cook DE, Thomma BPHJ. 2016. Chromatin biology impacts adaptive
716 evolution of filamentous plant pathogens. PLoS Pathog 12:e1005920.

717 37. Ridenour JB, Möller M, Freitag M. 2020. Polycomb repression without bristles:
718 facultative heterochromatin and genome stability in fungi. Genes (Basel) 11:638.

719 38. Fradin EF, Thomma BPHJ. 2006. Physiology and molecular aspects of Verticillium
720 wilt diseases caused by *V. dahliae* and *V. albo-atrum*. Mol Plant Pathol.

721 39. Klosterman SJ, Subbarao K V., Kang S, Veronese P, Gold SE, Thomma BPHJ, Chen
722 Z, Henrissat B, Lee YH, Park J, Garcia-Pedrajas MD, Barbara DJ, Anchieta A, de
723 Jonge R, Santhanam P, Maruthachalam K, Atallah Z, Amyotte SG, Paz Z,
724 Inderbitzin P, Hayes RJ, Heiman DI, Young S, Zeng Q, Engels R, Galagan J, Cuomo
725 CA, Dobinson KF, Ma LJ. 2011. Comparative genomics yields insights into niche
726 adaptation of plant vascular wilt pathogens. PLoS Pathog 7:e1002137.

727 40. de Jonge R, Bolton MD, Kombrink A, van den Berg GCM, Yadeta KA, Thomma
728 BPHJ. 2013. Extensive chromosomal reshuffling drives evolution of virulence in an
729 asexual pathogen. Genome Res 23:1271–1282.

730 41. Depotter JRL, Shi-Kunne X, Missonnier H, Liu T, Faino L, Berg GCM, Wood TA,
731 Zhang B, Jacques A, Seidl MF, Thomma BPHJ. 2019. Dynamic virulence-related
732 regions of the plant pathogenic fungus *Verticillium dahliae* display enhanced
733 sequence conservation. Mol Ecol doi: 10.1111/mec.15168.

734 42. Faino L, Seidl MF, Shi-Kunne X, Pauper M, Van Den Berg GCM, Wittenberg AHJ,
735 Thomma BPHJ. 2016. Transposons passively and actively contribute to evolution of
736 the two-speed genome of a fungal pathogen. Genome Res 26:1091–1100.

737 43. Shi-Kunne X, Faino L, van den Berg GCM, Thomma BPHJ, Seidl MF. 2018.
738 Evolution within the fungal genus *Verticillium* is characterized by chromosomal
739 rearrangement and gene loss. Environ Microbiol 20:1362–1373.

740 44. Cook DE, Kramer HM, Torres DE, Seidl MF, Thomma BPHJ. 2020. A unique
741 chromatin profile defines adaptive genomic regions in a fungal plant pathogen.
742 Elife 9:e62208.

743 45. Faino L, de Jonge R, Thomma BPHJ. 2012. The transcriptome of *Verticillium*
744 *dahliae*-infected *Nicotiana benthamiana* determined by deep RNA sequencing. Plant
745 Signal Behav 7:1065–1069.

746 46. Soyer JL, Möller M, Schotanus K, Connolly LR, Galazka JM, Freitag M, Stukenbrock
747 EH. 2015. Chromatin analyses of *Zymoseptoria tritici*: methods for chromatin
748 immunoprecipitation followed by high-throughput sequencing (ChIP-seq). Fungal
749 Genet Biol 79:63–70.

750 47. Buenrostro JD, Wu B, Chang HY, Greenleaf WJ. 2015. ATAC-seq: A method for
751 assaying chromatin accessibility genome-wide. Curr Protoc Mol Biol 2015:doi:
752 10.1002/0471142727.mb2129s109.

753 48. Schotanus K, Soyer JL, Connolly LR, Grandaubert J, Happel P, Smith KM, Freitag
754 M, Stukenbrock EH. 2015. Histone modifications rather than the novel regional
755 centromeres of *Zymoseptoria tritici* distinguish core and accessory chromosomes.
756 Epigenetics Chromatin 8:41.

757 49. Seidl MF, Kramer HM, Cook DE, Lorencini Fiorin G, van den Berg GCM, Faino L,

758 Thomma BPHJ. 2020. Repetitive elements contribute to the diversity and evolution
759 of centromeres in the fungal genus Verticillium. MBio 11:e01714-20.

760 50. Zhang W, Huang J, Cook DE. 2021. Histone modification dynamics at H3K27 are
761 associated with altered transcription of in planta induced genes in *Magnaporthe*
762 *oryzae*. PLoS Genet 17:e1009376.

763 51. Tang G, Yuan J, Wang J, Zhang Y-Z, Xie S-S, Wang H, Tao Z, Liu H, Kistler HC,
764 Zhao Y, Duan C-G, Liu W, Ma Z, Chen Y. 2021. *Fusarium* BP1 is a reader of H3K27
765 methylation. Nucleic Acids Res 49:10448–10464.

766 52. Wiles ET, McNaught KJ, Kaur G, Selker JML, Ormsby T, Aravind L, Selker EU. 2020.
767 Evolutionarily ancient BAH–PHD protein mediates Polycomb silencing. Proc Natl
768 Acad Sci 117:11614–11623.

769 53. Basenko EY, Sasaki T, Ji L, Prybol CJ, Burckhardt RM, Schmitz RJ, Lewis ZA. 2015.
770 Genome-wide redistribution of H3K27me3 is linked to genotoxic stress and
771 defective growth. Proc Natl Acad Sci 112:E6339–E6348.

772 54. Lewis ZA. 2017. Polycomb group systems in fungi: new models for understanding
773 polycomb repressive complex 2. Trends Genet 33:220–231.

774 55. Tralamazza SM, Abraham LN, Sarai Reyes-Avila C, Corrêa B, Croll D. 2021. Histone
775 H3K27 methylation perturbs transcriptional robustness and underpins
776 dispensability of highly conserved genes in fungi. Mol Biol Evol msab323.

777 56. Faino L, Seidl M, Datema E, van den Berg GCM, Janssen A, Wittenberg AHJ,
778 Thomma BPHJ. 2015. Single-molecule real-time sequencing combined with optical
779 mapping yields completely finished fungal genome. MBio 6:e00936-15.

780 57. Bray NL, Pimentel H, Melsted P, Pachter L. 2016. Near-optimal probabilistic RNA-
781 seq quantification. Nat Biotechnol 34:525–527.

782 58. Love MI, Huber W, Anders S. 2014. Moderated estimation of fold change and
783 dispersion for RNA-seq data with DESeq2. Genome Biol 15:550.

784 59. Martin M. 2011. Cutadapt removes adapter sequences from high-throughput
785 sequencing reads. EMBnet J 17:10–12.

786 60. Li H. 2013. Aligning sequence reads, clone sequences and assembly contigs with
787 BWA-MEM. arXiv:13033997.

788 61. Ramírez F, Dündar F, Diehl S, Grüning BA, Manke T. 2014. deepTools: a flexible
789 platform for exploring deep-sequencing data. Nucleic Acids Res 42:W187–W191.

790 62. Zerbino DR, Johnson N, Juettemann T, Wilder SP, Flicek P. 2014. WiggleTools:
791 parallel processing of large collections of genome-wide datasets for visualization
792 and statistical analysis. Bioinformatics 30:1008–1009.

793 63. Stovner EB, Sætrom P. 2019. Epic2 efficiently finds diffuse domains in ChIP-seq
794 data. Bioinformatics 35:4392–4393.

795 64. Santhanam P. 2012. Random insertional mutagenesis in fungal genomes to
796 identify virulence factors, p. 509–517. *In* Plant fungal pathogens. Springer.

797 65. Frandsen RJN, Andersson JA, Kristensen MB, Giese H. 2008. Efficient four fragment
798 cloning for the construction of vectors for targeted gene replacement in
799 filamentous fungi. BMC Mol Biol 9:70.

800